Abbreviated title: Dorsal and ventral stream interactions in parietal cortex

IN PRESS AT JOURNAL OF COGNITIVE NEUROSCIENCE

Temporal frequency tuning reveals interactions between the dorsal and ventral visual streams

Stephanie Kristensen[1,2], Frank E. Garcea[3,4], Bradford Z. Mahon[3,4,5,6], Jorge Almeida[1,2,*]

1. Faculty of Psychology and Educational Sciences, University of Coimbra, 3001-802 Coimbra, Portugal
2. Proaction laboratory, Faculty of Psychology and Educational Sciences, University of Coimbra, 3001-802 Coimbra, Portugal.
3. Department of Brain and Cognitive Sciences, University of Rochester, Rochester, NY 14627-0268, USA
4. Center for Visual Science, University of Rochester, Rochester, NY 14627-0268, USA.
5. Department of Neurosurgery, University of Rochester, Rochester, NY 14627-0268, USA.
6. Department of Neurology, University of Rochester, Rochester, NY 14627-0268, USA.

* Correspondence should be sent to:

Jorge Almeida,

Faculty of Psychology and Educational Sciences,

University of Coimbra

3001-802 Coimbra, Portugal.

Email: jorgealmeida@fpce.uc.pt

CONFLICTS OF INTEREST: The authors declare no competing financial interests.

ACKNOWLEDGEMENTS: This work was supported by a Foundation for Science and Technology of Portugal Project Grant PTDC/MHC-PCN/3575/2012 and *programa COMPETE* to JA. SK was supported by a research initiation grant from the Foundation for Science and Technology of Portugal Project Grant PTDC/MHC-PCN/3575/2012. Preparation of this ms was supported in part by NIH grant R01 NS089609 to BZM. FEG was supported by a University of Rochester Center for Visual Science pre-doctoral training fellowship (NIH training grant 5T32EY007125-24).

ABSTRACT

Visual processing of complex objects is supported by the ventral visual pathway in the service of object identification and by the dorsal visual pathway in the service of object-directed reaching and grasping. Here we address how these two streams interact during tool processing, by exploiting the known asymmetry in projections of subcortical magnocellular and parvocellular inputs to the dorsal and ventral streams. The ventral visual pathway receives both parvocellular and magnocellular input, while the dorsal visual pathway receives largely magnocellular input. We used fMRI to measure tool preferences in parietal cortex when the images were presented at either high or low temporal frequencies, exploiting the fact that parvocellular channels project principally to the ventral but not the dorsal visual pathway. We reason that regions of parietal cortex that exhibit tool preferences for stimuli presented at frequencies characteristic of the parvocellular pathway receive their inputs from the ventral stream. We found that the left inferior parietal lobule, in the vicinity of the supramarginal gyrus, exhibited tool preferences for images presented at low temporal frequencies, whereas superior and posterior parietal regions exhibited tool preferences for images present at high temporal frequencies. These data indicate that object identity, processed within the ventral stream, is communicated to the left inferior parietal lobule, and may there combine with inputs from the dorsal visual pathway to allow for functionally appropriate object manipulation.

1. INTRODUCTION

Visual object processing can be separated into two distinct streams: a ventral stream, projecting from primary visual cortex (V1) to ventro-temporal regions, responsible for object identification, and a dorsal stream, projecting to posterior parietal cortex, responsible for the processing of object-directed actions and visuomotor control (e.g., Goodale & Milner, 1992). The dorsal stream can be further separated into a dorso-dorsal stream, including the superior parietal lobe, focused on online visuomotor control of actions, and a ventro-dorsal stream, including the inferior parietal lobe, critical for the representation of complex actions (Rizzolatti & Mattelli, 2003; see also & Binkofski & Buxbaum, 2013).

Object recognition and optimal visuomotor interactions with objects require information from both the ventral and dorsal streams to be brought into register. In particular, using an object correctly according to its function requires access to the visuomotor computations performed over the volumetric properties of that object, typical of the dorsal stream, as well as access to ventral stream information regarding the identity of the target object, and its canonical function. Exactly how those distinct types of information are integrated remains unclear. Here we will focus on where in the left parietal lobule these channels of information interact during visual processing of manipulable objects (i.e., tools).

Vision is a highly segregated system, and two main subcortical pathways have been consistently demonstrated – the magnocellular (M) and parvocellular (P) pathways – that separate already in the retina. Retinal midget ganglion cells project to parvocellular layers of the lateral geniculate nucleus (LGN), whereas retinal parasol ganglion cells project to the magnocellular layers of the LGN (e.g., Livingston & Hubel 1988). Importantly, magnocellular and parvocellular pathways project differentially to the ventral and dorsal streams. The parvocellular pathway projects mainly to regions within the ventral stream, whereas the

magnocellular pathway projects to both dorsal and ventral stream regions (Ferrera, Nealey, & Maunsell, 1992; Merigan & Maunsell, 1993).

This asymmetry in the projection of magnocellular and parvocellular inputs to the dorsal and ventral streams can be leveraged to test where the two streams come into register. Specifically, if we see signatures of parvocellular processing within regions of parietal cortex, then that would suggest that those parietal regions receive information from the ventral (and not the dorsal) visual pathway (for prior work within this framework, see Almeida et al., 2013; Mahon et al., 2013). In this study we capitalize on the fact that magnocellular and parvocellular pathways have distinct temporal frequency preferences: magnocellular cells have high temporal resolution allowing them to detect stimuli at high temporal frequencies (such as flickering or fast motion), with highest sensitivity at temporal frequencies between 10 and 20Hz (Derrington and Lennie, 1984). In comparison, parvocellular cells have a sustained response pattern and thus show a preference for slow-moving or static stimuli and respond more strongly to stimuli at lower temporal frequencies up to 10Hz with a very steep decrease in the ability to respond to frequencies at and above 10 Hz (Derrington & Lennie, 1984; Livingstone and Hubel, 1988). As such, temporal frequencies below 10 Hz (Low Temporal Frequencies – LTF) are better processed by the parvocellular pathway, whereas temporal frequencies above 10 Hz (and especially between 10 and 20 Hz; High Temporal Frequencies – HTF) are resolvable by the magnocellular pathway. Those temporal frequency preferences, initially established in the macaque, have also recently been shown to obtain in the human brain. Denison and colleagues (Denison, Vu, Yacoub, Feinberg, and Silver, 2014) demonstrated that using visual stimuli flickering at 5 and 15Hz elicited responses in the P and M layers of the human LGN respectively.

Experiment

In our experiment we presented sequences of pictures of tools or animals at different presentation rates. Specifically, we presented pictures at low temporal frequencies or at high temporal frequencies in order to differentially excite the parvocellular and magnocellular pathways, respectively. We then tested how tool preferences within parietal areas are modulated by the temporal frequency at which the stimuli were presented. If we see areas within parietal cortex that respond more to tool items than control (i.e., animal) items when these items are presented at low temporal frequencies typical of parvocellular pathways, then we can conclude that those areas receive their inputs by way of a ventral visual pathway analysis of the input and not a dorsal visual pathway analysis.

2. EXPERIMENTAL PROCEDURES

2.1 Participants.

20 participants were tested, of which 19 completed 8 experimental runs and one 6 runs (14 female). All participants were right-handed, had normal or corrected to normal vision, and no history of neurological disorders. The project was approved by the ethical committee of the Faculty of Medicine, University of Coimbra.

2.2 Experimental stimuli.

Stimuli were greyscale pictures of animals and tools. Twelve animal and twelve tool items were used, with twenty exemplars for each item (total of 480 pictures). The stimuli were 400x400 pixels in size (~10° of visual angle) and were presented on a grey background, using an Avotec projector under 60 Hz refresh rate. Colored images were collected from the World Wide Web and internal image databases. Items used were as follows: animals: bear, cat, cow, dog, horse, owl, panda, pigeon, rabbit, raccoon, sheep, tiger; tools: bat, broom, corkscrew, flashlight, flyswatter, hammer, paintbrush, pen, scissors, screwdriver, shovel, and stapler.

2.3 General Procedure.

"A simple framework" (Schwarzbach, 2011) was used to control stimulus presentation in Psychtoolbox in MATLAB running on Windows 7 (Brainard, 1997). Stimuli were back-projected on a screen that participants viewed with a mirror attached to the head coil. Participants viewed the tool and animal stimuli passively (no response) in a miniblock design. Our design consisted of 2 categories (animals and tools) x 4 presentation rates (5, 10, 15, 30Hz) for a total of 8 conditions. Each miniblock represented one cell of the design and lasted 8 seconds. Miniblocks of stimuli were separated by 8 sec of fixation. The 240 items for each category were repeated twice within the design: each image from a given category was presented once in the 30Hz condition (all 240 items) condition, and once again across the remaining three conditions (40 items in the 5Hz, 80 items in the 10Hz, and 120 items in the 15Hz condition). Miniblocks were then pseudo-randomized within each run so that no more than 2 miniblocks of the same category occurred consecutively. Each run contained 2 repetitions of the design, or 16 miniblocks in total, and lasted approximately 4 minutes and 40 seconds. The speeds of 5, 10, 15, and 30Hz corresponded to image presentation durations of 200 ms, 100 ms, 67 ms, and 33 ms per image, respectively. Between either runs 3 and 4, or runs 4 and 5, participants completed an experimental run to map population receptive fields (data not reported herein).

2.4 MRI Parameters.

Whole-brain BOLD imaging was conducted on a Siemens Tim Trio 3T MRI scanner with a 12-channel head coil at the Portuguese Brain Imaging Network. High-resolution structural T1 contrast images were acquired using a magnetization prepared rapid gradient-echo pulse sequence at the start of each session (repetition time=2530msec, echo time=3.29msec, flip angle=7°, field of view=256mm, matrix=256×256, 1×1×1mm ascending

interleaved slices). An EPI pulse sequence was used for T2* contrast (repetition time=2000msec, echo time= 30 msec, flip angle=90°, field of view=256 mm, matrix 256x256, 30 ascending interleaved even-odd slices, voxel size=1x1x1 mm). The first two volumes of each run were discarded to allow for signal equilibration.

2.5 fMRI Data Analysis.

fMRI data were analyzed with the Brain Voyager software package 2.8.1 and in-house scripts drawing on the BVQX toolbox for MATLAB. Preprocessing of the functional data included, in the following order, slice time correction (sinc interpolation), motion correction with respect to the first volume of the first functional run, and linear trend removal in the temporal domain (cutoff: two cycles within the run). Functional data were registered (after contrast inversion of the first volume) to high-resolution deskulled anatomy on a participant-by-participant basis in native space. For each participant, echo-planar and anatomical volumes were transformed into standardized (Talairach & Tournoux, 1988) space. Functional data were smoothed at 6-mm (1.5 voxels) FWHM and interpolated to 3 × 3 × 3 mm voxels. The general linear model was used to fit beta estimates to the events of interest. The first derivatives of 3-D motion correction from each run were added to all models as regressors of no interest to attract variance attributable to head movement. All analyses treated participants as a random factor, and there were thus 19 degrees of freedom in the group-level analyses. Experimental events were convolved with a standard two-gamma hemodynamic response function. There were 8 (2 × 4) regressors: the category of the stimulus (tools and animals) and the presentation rate of images (5, 10, 15, and 30 Hz).

We computed an ANOVA with two within-participant factors: Category (Tool vs Animal) and Presentation Rate (5 Hz, 10 Hz, 15 Hz and 30 Hz). From this, we inspected left parietal cortex for regions exhibiting an interaction between these two factors. We then focused

on testing the simple effects, and computed four contrasts in order to look for stronger neural activation for tools than animals at each presentation rate. Based on the prior literature in humans (Denison et al., 2014) we then focused on 2 of those simple contrasts: we focused on tool preferences by comparing neural activation for tools and animals when both stimulus types were presented at temporal frequencies within the parvocellular response spectrum ([$Tools_{[5Hz]}$ > $Animals_{[5Hz]}$]) or within the magnocellular response spectrum ([$Tools_{[15Hz]}$ > $Animals_{[15Hz]}$]).

3. RESULTS

Inferior-to-superior organization of tool preferences by temporal frequency within parietal cortex.

We first conducted a two-way ANOVA with Category (Tool vs. Animals) and Presentation rate (5 Hz, 10 Hz, 15 Hz, and 30 Hz) as within participant factors to test whether responses within left parietal cortex to tool items, compared to animal items, were dependent on the presentation rate at which the target pictures were presented. Figure 1A shows the activation map obtained for the interaction between those two factors (cluster corrected at $p \leq 0.05$). As can be seen in this Figure, an extensive left parietal area was obtained, spanning parts of the inferior parietal lobule (namely the supramarginal gyrus), and superior parietal lobule, as well as parts of the intraparietal sulcus.

We then tested tool preferences within each presentation rate and computed 4 simple effects contrasting tools with animals for each speed (5, 10, 15 and 30 Hz). As can be seen in Figure 1B (all maps thresholded at FDR $q < .05$), tools elicited stronger activity in medial aspects of the left fusiform gyrus under all presentation rates. However, there were differences in how parietal cortex responded to tools (when compared to animals) at the different speeds. In particular, certain speeds elicited tool specific activity within more superior aspects of

parietal cortex (i.e., the simple contrasts for 10 and 15Hz), or in more inferior aspects (i.e, the simple contrasts for 5Hz), or failed to elicit any differential activity (i.e, the simple contrasts for 30Hz).

Importantly, because we were interested in how different regions within tool-sensitive parietal cortex processed M and P-biased input, we focused on characterizing tool preferences under M and P-related speeds. For this, we further inspected the simple effects that have previously been established as optimal for eliciting P-biased and M-biased processing, and tested these simple effects (Tools > Animals) within the parietal region obtained from our ANOVA. For the P-Biased Tool contrast, because the parvocellular pathway prefers low temporal frequencies below 10 Hz, we inspected tool preferences (i.e., voxels presenting higher activation for tools when compared to animals) when all stimuli (tools and animals) were presented at 5Hz (see also Denison et al., 2014). To identify tool preferences that are communicated via the magnocellular-dominated dorsal stream, and because the magnocellular pathway prefers high temporal frequencies, in particular between 10 and 20 Hz, we explored tool preferences when all stimuli were presented at 15Hz (see also Denison et al., 2014). Importantly, these contrasts, which show tool preferences separately for high and low temporal frequencies, are entirely independent from one another—thus there is nothing about this analysis approach that would bias against observing completely overlapping voxels as exhibiting tool preferences for 5Hz and 15Hz presentation rates.

The left parietal region presented in Fig. 1A was sliced into 3 mm thick planes along the inferior-to-superior plane (i.e., along the z-dimension) to capture the divide between superior and inferior aspects of parietal cortex. We treated each slice as a separate region of interest and extracted the *t*-values for each of our 2 simple contrasts (([$\text{Tools}_{[5\text{Hz}]}$ > $\text{Animals}_{[5\text{Hz}]}$], and [$\text{Tools}_{[15\text{Hz}]}$ > $\text{Animals}_{[15\text{Hz}]}$]). These *t*-values were compared in order to ascertain whether at each slice along the inferior-to-superior dimension, tool preferences presented different biases

(i.e., M and P). As can be seen in Figure 1C, there is a clear divide in the M and P biases for the slices below and above z = 46/49, which corresponds well with the approximate location of the anterior intraparietal sulcus (for review see Garcea and Mahon, 2014). Below z = 46/49, *t*-values for the simple effect of tools over animals under low temporal frequencies (5 Hz) are, on average, greater than those for tool preferences under high temporal frequencies (15 Hz); above z = 46/49 *t*-values for low temporal frequency dependent tool preferences tended to be, on average, less than those for high temporal frequency dependent tool preferences.

We then further inspected these M and P simple effects at the whole-brain level. The resulting contrast maps, corrected for multiple comparisons using a false discovery rate of 5% (i.e., all maps thresholded at FDR $q < .05$), are shown in Figure 2A. There were largely nonoverlapping regions of left parietal cortex responding differently to these two contrasts. Tool preferences for low temporal frequency presentations were observed in more inferior aspects of left parietal cortex principally within BA40 (i.e., the supramarginal gyrus), whereas tool preferences for high temporal frequency presentations were observed in superior (i.e., BA7) and posterior aspects of left parietal cortex. These findings are in extremely good agreement with prior work indicating an inferior-to-superior dissociation in left parietal tool preferring regions by subcortical distinctions (Almeida, Fintzi, & Mahon, 2013; Mahon, Kumar, & Almeida, 2013). In that prior work, we observed a very similar inferior-to-superior organization whereby inferior parietal regions exhibited tool preferences for stimuli defined by high spatial frequencies (Mahon et al., 2013) or isoluminant chromatic (red/green) information (Almeida et al., 2013). The current findings, using temporal frequencies, converge with those prior findings to indicate that tool preferences in the left inferior parietal lobule are contingent on analysis of the visual input by the ventral visual pathway.

Finally, we sought to compare how the regions we showed to be dependent on low or high temporal frequencies fared with known anatomical and functional parcellations of parietal

cortex (e.g., Caspers et al. 2006, 2008; Choi et al., 2006; Scheperjans 2008a, 2008b). First, we wanted to understand whether and how our interaction region and our contrasts of interest overlapped. Figure 2B shows a considerable amount of overlap between the two contrasts and the region of interest obtained for the interaction between the category of the stimuli and the presentation rate at which the stimuli were presented. More importantly, Figure 2C shows the overlap of our contrasts of interest with the parcellations proposed by Caspers and colleagues for the inferior parietal lobule (2006, 2008). According to Caspers and colleagues, the supramarginal gyrus encompasses 5 sub regions that span this region across the posterior-to-anterior dimension: PFm, PF, PFcm, PFt and PFop. Interestingly, our low temporal frequency, P-biased tool-preferring region overlaps maximally with area PFt and to a much lesser extent with area PF; in contrast, our high temporal frequency, M-biased tool-preferring regions show no overlap with any of the clusters within the supramarginal gyrus. Interestingly, PFt has been shown to be anatomically connected, amongst other areas, to anterior and posterior fusiform gyrus, regions within the intraparietal sulcus and superior parietal areas (Caspers et al., 2011). Moving superiorly, Scheperjans and colleagues (2008a; 2008b), and Choi and colleagues (2006) subdivided the human intraparietal sulcus into three regions: hIP1, hIP2, and hIP3. As can be seen in Figure 2D, there is not a lot of overlap between those parcellations and our contrasts. If anything, our P-biased tool preferences overlap minimally with the inferior lateral bank of the intraparietal sulcus around region hIP2, whereas our M-biased tool preferences overlapped with the superior aspect in the vicinity of hIP3. Finally, we also tested the overlap of our contrasts with clusters within the superior parietal lobule, and specifically within BA 7. According to Scheperjans and colleagues (2008a; 2008b), this Brodmann area can be further parcellated into 4 clusters: 7A, 7P, 7PC, and 7M. Figure 2E shows that our M-biased tool contrast overlaps with areas 7A, P and PC, whereas our P-biased tool contrast shows no overlap with any of these clusters.

It is important to note that these M and P simple effects show pathway-biased tool preferences extend somewhat beyond the parietal region that was defined by the interaction between presentation rate and category (see Figures 1A and 2B). Nevertheless, it seems clear that the major results presented here still hold, albeit in a more spatially circumscribed fashion, even if we look only at the sites where the M and P simple contrasts and the interaction region overlap. That is, P-biased tool preferences are present in the PFt region within the supramarginal gyrus, and in parts of the hIPS (i.e., hIP2), whereas M-biased tool preferences are limited to areas within BA7 (i.e., 7A and 7PC).

4. DISCUSSION

Here we reported evidence that tool preferences in the inferior parietal lobule are contingent on inputs from the ventral visual pathway. We used images of tools and animals and presented them at different temporal frequencies to bias processing either toward the magnocellular or parvocellular pathways. The parvocellular pathway has greater sensitivity for low temporal frequencies, and projects to the ventral visual pathway, whereas the magnocellular pathway has greater sensitivity for high temporal frequencies and projects to both the dorsal and ventral streams. Thus, in the measure to which tool preferring regions of parietal cortex show stronger tool preferences for low temporal frequencies, it can be concluded that those regions receive their inputs from the ventral visual pathway. We found that tool preferences under low temporal frequencies were restricted to the inferior parietal lobule, namely within area PFt (a region within the supramarginal gyrus), whereas tool preferences under high temporal frequencies were present within the superior parts of the parietal lobe, namely regions 7A, P, and PC within BA 7, and more posterior aspects of parietal cortex. Because the parvocellular pathway projects to ventral and not dorsal stream structures, the observation that tool preferences in the inferior parietal lobule are carried by low temporal frequencies indicates that the inferior parietal lobule receives inputs during visual processing of tools from the ventral

visual pathway. This does not preclude our low temporal frequency tool preferring area from receiving M-biased information. As a matter of fact, the subdivision where our area lies – the ventro-dorsal stream – receives input from area MT/V5, a region that receives magnocellular input (Lyon et al., 2010). It seems, however, that when filtered through the constraint of exhibiting differential BOLD responses to tools compared to animals, there is a clear bias whereby the major input originates from P-biased ventral stream structures.

It is important to note, that the seminal studies demonstrating different temporal frequency profiles for M and P pathways were conducted using very simple stimuli (i.e., gratings) and in non-human animals (e.g., Owl Monkey, Xu et al., 2001), whereas here we use complex objects, and measured neural activity in humans. Importantly, Denison and Colleagues (Denison et al., 2014) demonstrated that the P and M layers of the human LGN are also excited by low and high temporal frequencies respectively – notably the frequencies used by Denison and Colleagues were the same as our frequencies of interest. Moreover, there are many differences between our high and low temporal frequency conditions (e.g., number of pictures presented in each condition) and between our categories of interest (e.g., tools are elongated whereas most animals are not). Some of these differences were also true, however, for the experiments performed over simple stimuli (e.g., the number of alternations between the phases of the gratings used to separate M and P responses were necessarily different for high and low temporal frequencies, as they were for our low and high temporal frequency sequences of pictures). Interestingly, other aspects that differ between our conditions should be explicitly addressed in future work, namely the issue of elongation and how object elongation may be a basic feature that biases processing of a complex object within the ventral and dorsal streams (Almeida, 2010; Almeida et al., 2014; Sakuraba, Sakai, Yamanaka, Yokosawa, & Hirayama, 2012).

Our findings are in line with those previously obtained by our group (Almeida et al., 2013; Mahon et al., 2013). Those studies explored how other neurophysiological characteristics of the same subcortical pathways affected tool preferences in parietal cortex. Specifically, those studies found that stimuli that contained only high spatial frequencies (Mahon et al., 2013), or were defined by isoluminant red/green differences (Almeida et al., 2013), led to tool preferences restricted to the left inferior parietal lobule. In contrast, tool preferences in superior and posterior parietal cortex were driven by low spatial frequencies (Mahon et al., 2013) and color distinctions (blue/yellow) carried by non-parvocellular pathways (e.g., the koniocellular pathway; Almeida et al., 2013). The results we have reported herein, together with those prior studies, shed new light on the interaction between the dorsal and ventral visual streams, as they illustrate that the computations occurring within the left inferior parietal lobule, presumably related to object manipulation knowledge (Boronat et al., 2005; Chen, Garcea and Mahon, 2015; Ishibashi, Lambon Ralph, Saito, & Pobric, 2011; Kellenbach, Brett, & Patterson, 2003; Mahon et al., 2007), are contingent on analysis of the visual input by the ventral visual pathway (see also Binkofski & Buxbaum, 2013; Garcea & Mahon, 2014).

The data herein may be a manifestation of an important distinction proposed by Johnson & Grafton (2003) on the difference between *acting on* an object and *acting with* an object. Acting *on* an object refers to interacting with an object by treating the object as a manipulable entity, devoid of particular functions and manipulations, but focusing on the visuomotor aspects of the object such as its volumetric properties and its spatial relation with the effector. Acting *with* an object refers to exploiting the object's typical function and associated manner of manipulation, in the service of a goal. Interestingly, regions within the superior parietal lobule (and in the vicinity of our M-biased tool region) are of central importance for the kinds of processing that subserve *acting on* an object. For instance, this M-biased tool region shows some overlap with areas within parietal cortex that are responsible for extracting and computing

3D shape (e.g., DIPSM, DIPSA, and POIPS; Durand et al., 2009; Georgieva et al, 2008, 2009; Orban et al., 2003), perhaps suggesting a role in processing volumetric properties such as 3D shape in the service of preparing a grasp and planning to manipulate an object. Regions within the inferior parietal lobule (and in the vicinity of our P-biased tool region) support the processes that are at play when *acting with* objects (Brandi, Wohlschläger, Sorg, & Hermsdörfer, 2014; Binkofski & Buxbaum, 2013; Rizolatti & Matelli, 2003). Clearly, these data also seem to map onto the proposed subdivision of the dorsal pathway into dorso-dorsal and ventro-dorsal streams (Binkofski & Buxbaum, 2013; Rizolatti & Matelli, 2003).

So how does our tool-selective region, that is contingent upon the processing happening within the ventral stream, fit with the proposal of Johnson & Grafton (2003)? There seems to be overlap between our P-biased tool-preferring regions, and those reported by Brandi and colleagues (Brandi, Wohlschläger, Sorg, & Hermsdörfer, 2014) and Peeters and colleagues (e.g., Peeters, Rizzolatti, & Orban,, 2013). Those foci of activity are within the anterior parts of the supramarginal gyrus, more specifically in or around area PFt. Importantly, PFt seems to be coding aspects that are specific to tool-related actions, and not overall hand actions, and be related with overlearned, function-specific, manipulations of familiar tools (e.g., Brandi et al., 2014; Peeters et al., 2013). Our data further chart the complex processing within this region by demonstrating that this information is dependent on the processing happening within the ventral stream. This may be so, potentially, because of the need to retrieve the actual function of the object in order to map the associated manipulation, and therefore implement the causal relationship between function, manipulation and consequential use of a tool. This is also in line with the findings of Valyear and Culham (2010) that showed that neural responses to hand grasps that are contingent on the typical use of an object are obtained within ventral stream regions. Our data may also point to the fact that processing within the ventral stream facilitates the understanding of the technical properties that a target tool possesses (e.g., a sharp toothed

resistant surface), and that can be used to fulfill certain goals (e.g., to cut; e.g., Osiurak, Jarry, & Le Gall, 2010).

More generally, the above considerations are in line with the suggestion that abstract information may be integrated with motor plans within the inferior parietal lobule (e.g. Arbib, 2008). The left inferior parietal lobule has long been associated with the planning of gestures and actions for tool use (e.g., Johnson-Frey, Newman-Norlund, & Grafton, 2005; Vingerhoets, Acke, van Demaele, & Achten, 2009). Buxbaum, Kyle, Grossman, and Coslett (2007) and Arbib (2008) suggested that the inferior parietal lobule functions as an area of integration between object identity information from the ventral stream and spatial body representations processed within the dorsal stream. Possibly, this integration plays a major role in the selection and preparation of the appropriate motor manipulation when reaching towards objects. For example, consider reaching for a pen. Appropriate grasping of a pen will be dependent not only on the shape of the pen, but also on the action to be executed. Picking up the pen for writing will elicit a different grasp compared to picking up the pen in order to pass it to someone. The left inferior parietal lobule has the connectivity and response characteristics to compute grasp information that is informed by the (often implicit) planned or anticipated use of the object.

REFERENCES

Almeida, J. (2010). *Unconscious processes reveal different circuits for visual object recognition*. Harvard University, Cambridge MA.

Almeida, J., Fintzi, A. R., & Mahon, B. Z. (2013). Tool manipulation knowledge is retrieved by way of the ventral visual object processing pathway. *Cortex, 49*(9), 2334–2344. doi:http://dx.doi.org/10.1016/j.cortex.2013.05.004

Almeida, J., Mahon, B., Zapater-Raberov, V., Dziuba, A., Cabaço, T., Marques, J.F., & Caramazza, A. (2014). Grasping with the eyes: the role of elongation in visual recognition of manipulable objects. *Cognitive, Affective and Behavioral Neuroscience, 14*(1), 319-335.

Arbib, M. A. (2008). From grasp to language: embodied concepts and the challenge of abstraction. *Journal of Physiology, Paris*, *102*(1-3), 4–20. doi:10.1016/j.jphysparis.2008.03.001

Binkofski, F., & Buxbaum, L. J. (2013). Two action systems in the human brain. *Brain and Language*, *127*(2), 222–9. doi:10.1016/j.bandl.2012.07.007Boronat, C. B., Buxbaum, L. J., Coslett, H. B., Tang, K., Saffran, E. M., Kimberg, D. Y., & Detre, J. A. (2005). Distinctions between manipulation and function knowledge of objects: evidence from functional magnetic resonance imaging. *Brain Research. Cognitive Brain Research*, *23*(2-3), 361–73. doi:10.1016/j.cogbrainres.2004.11.001

Brandi, M.-L., Wohlschläger, A., Sorg, C., & Hermsdörfer, J. (2014). The neural correlates of planning and executing actual tool use. *Journal of Neuroscience*, *34*(39), 13183–13194. doi:10.1523/JNEUROSCI.0597-14.2014

Brainard, D.H. (1997) The Psychophysics Toolbox. *Spatial Vision, 10*, 433-436.

Buxbaum, L. J., Kyle, K., Grossman, M., & Coslett, B. (2007). Left Inferior Parietal Representations for Skilled Hand-Object Interactions: Evidence from Stroke and Corticobasal Degeneration. *Cortex*, *43*(3), 411–423. doi:10.1016/S0010-9452(08)70466-0

Caspers, S., Eickhoff, S. B., Geyer, S., Scheperjans, F., Mohlberg, H., Zilles, K., & Amunts, K. (2008). The human inferior parietal lobule in stereotaxic space. *Brain Structure and Function*, *212*(6), 481–495. doi:10.1007/s00429-008-0195-z

Caspers, S., Eickhoff, S. B., Rick, T., von Kapri, A., Kuhlen, T., Huang, R., Shah, N.J., & Zilles, K. (2011). Probabilistic fibre tract analysis of cytoarchitectonically defined human inferior parietal lobule areas reveals similarities to macaques. *Neuroimage, 58*(2), 362-380.

Caspers, S., Geyer, S., Schleicher, A., Mohlberg, H., Amunts, K., & Zilles, K. (2006). The human inferior parietal cortex: Cytoarchitectonic parcellation and interindividual variability. *NeuroImage*, *33*(2), 430–448. doi:10.1016/j.neuroimage.2006.06.054

Chen, Q., Garcea, F.E., & Mahon, B.Z. (2015). The representation of object-directed action 10.1093/cercor/bhu328 and function knowledge in the human brain. *Cerebral Cortex*. Epub ahead of print. 10.1093/cercor/bhu328.

Choi, H.-J., Zilles, K., Mohlberg, H., Schleicher, A., Fink, G. R., Armstrong, E., & Amunts, K. (2006). Cytoarchitectonic identification and probabilistic mapping of two distinct areas within the anterior ventral bank of the human intraparietal sulcus. *The Journal of Comparative Neurology*, *495*(1), 53–69. doi:10.1002/cne.20849

Denison, R.N., Vu, A.T., Yacoub, E., Feinberg, D.A., & Silver, M.A. (2014). Functional mapping of the magnocellular and parvocellular subdivisions of human LGN. *Neuroimage, 102*, 358-369.

Derrington, M., & Lennie, P. (1984). Spatial and temporal contrast sensitivities of neurones in lateral geniculate nucleus of macaque. *The Journal of Physiology*, *357*, 219–40.

Durand, J-B., Peeters, R., Norman, F., Todd, J.T. & Orban, G.A. (2009). Parietal regions processing visual 3D shape extracted from disparity. *NeuroImage, 46*, 1114–1126.

Eickhoff, S. B., Stephan, K. E., Mohlberg, H., Grefkes, C., Fink, G. R., Amunts, K., & Zilles, K. (2005). A new SPM toolbox for combining probabilistic cytoarchitectonic maps and functional imaging data. *NeuroImage*, *25*(4), 1325–1335. doi:10.1016/j.neuroimage.2004.12.034

Ferrera, V. P., Nealey, T. A., & Maunsell, J. H. R. (1992). Mixed parvocellular and magnocellular geniculate signals in visual area V4. *Nature*, *358*(6389), 756–758. Retrieved from http://dx.doi.org/10.1038/358756a0

Garcea, F. E., & Mahon, B. Z. (2014). Parcellation of left parietal tool representations by functional connectivity. *Neuropsychologia*, *60*, 131–43. doi:10.1016/j.neuropsychologia.2014.05.018

Georgieva, S., Peeters, R., Kolster, H., Todd, J.T. & Orban, G.A. (2009). The processing of three dimensional shape from disparity in the human brain. *Journal of Neuroscience, 29*, 727–742.

Georgieva, S.S., Todd, J.T., Peeters, R. & Orban, G.A. (2008). The extraction of 3D shape from texture and shading in the human brain. *Cerebral Cortex, 18*, 2416–2438.

Goodale, M. A., & Milner, A. D. (1992). Separate visual pathways for perception and action. *Trends in Neurosciences*, *15*(1), 20–25. doi:http://dx.doi.org/10.1016/0166-2236(92)90344-8

Ishibashi, R., Lambon Ralph, M. A., Saito, S., & Pobric, G. (2011). Different roles of lateral anterior temporal lobe and inferior parietal lobule in coding function and manipulation tool knowledge: evidence from an rTMS study. *Neuropsychologia*, *49*(5), 1128–35. doi:10.1016/j.neuropsychologia.2011.01.004

Johnson-Frey, S. H., Newman-Norlund, R., & Grafton, S. T. (2005). A distributed left hemisphere network active during panning of everyday tool use skills. *Cerebral Cortex*, *15*(6), 681–695. doi:10.1093/cercor/bhh169

Kellenbach, M.L., Brett, M., Patterson, K. (2003). Actions speak louder than functions: The importance of manipulability and action in tool representation. *Cognitive Neuroscience, 15,* 30–46.

Livingstone, M., & Hubel, D. (1988). Segregation of form, color, movement, and depth: anatomy, physiology, and perception. *Science*, *240*(4853), 740–749. doi:10.1126/science.3283936

Lyon, D.C., Nassi, J. J., Callaway, E.M. (2010). A Disynaptic Relay from Superior Colliculus to Dorsal Stream Visual Cortex in Macaque Monkey, *Neuron*, 65, 270-279.

Mahon, B. Z., Kumar, N., & Almeida, J. (2013). Spatial frequency tuning reveals interactions between the dorsal and ventral visual systems. *Journal of Cognitive Neuroscience*, *25*(6), 862–71. doi:10.1162/jocn_a_00370

Merigan, W. H., & Maunsell, J. H. R. (1993). How parallel are the primate visual pathways? *Annual Review of Neuroscience*, *16*(1), 369–402. doi:10.1146/annurev.ne.16.030193.002101

Orban, G. A., Fize, D., Peuskens, H., Denys, K., Nelissen, K., Sunaert, S., et al. (2003). Similarities and differences in motion processing between the human and macaque brain: Evidence from fMRI. *Neuropsychologia, 41*, 1757–1768.

Osiurak, F., Jarry, C., & Le Gall, D. (2010). Grasping the affordances, understanding the reasoning: toward a dialectical theory of human tool use. *Psychological Review*, *117*(2), 517–540. doi:10.1037/a0019004

Peeters, R. R., Rizzolatti, G., & Orban, G. A. (2013). Functional properties of the left parietal tool use region. *NeuroImage*, *78*(August 2015), 83–93. doi:10.1016/j.neuroimage.2013.04.023

Rizzolatti, G., & Matelli, M. (2003). Two different streams form the dorsal visual system: anatomy and functions. *Experimental Brain Research*, *153*(2), 146–157. doi:10.1007/s00221-003-1588-0

Sakuraba, S., Sakai, S., Yamanaka, M., Yokosawa, K., & Hirayama, K. (2012). Does the human dorsal stream really process a category for tools? *The Journal of Neuroscience : The Official Journal of the Society for Neuroscience*, *32*(11), 3949–53. doi:10.1523/JNEUROSCI.3973-11.2012

Scheperjans, F., Eickhoff, S. B., Hömke, L., Mohlberg, H., Hermann, K., Amunts, K., & Zilles, K. (2008a). Probabilistic maps, morphometry, and variability of cytoarchitectonic

areas in the human superior parietal cortex. *Cerebral Cortex*, *18*(9), 2141–2157. doi:10.1093/cercor/bhm241

Scheperjans, F., Hermann, K., Eickhoff, S. B., Amunts, K., Schleicher, a., & Zilles, K. (2008b). Observer-independent cytoarchitectonic mapping of the human superior parietal cortex. *Cerebral Cortex*, *18*(4), 846–867. doi:10.1093/cercor/bhm116

Schwarzbach, J. (2011). A simple framework (ASF) for behavioral and neuroimaging experiments based on the psychophysics toolbox for MATLAB. *Behavior Research Methods*, *43*(4), 1194–1201. doi:10.3758/s13428-011-0106-8

Talairach, P., & Tournoux, J. (1988). A stereotactic coplanar atlas of the human brain. Stuttgart: Thieme.

Valyear, K. F., & Culham, J. C. (2010). Observing Learned Object-specific Functional Grasps Preferentially Activates the Ventral Stream. *Journal of Cognitive Neuroscience*, *22*(5), 970–984. http://doi.org/10.1162/jocn.2009.21256

Vingerhoets, G., Acke, F., Vandemaele, P., & Achten, E. (2009). Tool responsive regions in the posterior parietal cortex: Effect of differences in motor goal and target object during imagined transitive movements. *NeuroImage*, *47*(4), 1832–1843. doi:http://dx.doi.org/10.1016/j.neuroimage.2009.05.100

Xu, X., Ichida, J. M., Allison, J. D., Boyd, J. D., Bonds, A. B., & Casagrande, V. A. (2001). A comparison of koniocellular, magnocellular and parvocellular receptive field properties in the lateral geniculate nucleus of the owl monkey (Aotus trivirgatus). *Journal of Physiology*, *531*(1), 203–218. doi:10.1111/j.1469-7793.2001.0203j.x

Figure 1. Inferior-to-superior organization of left parietal cortex by temporal frequency dependent tool-preferences. A) Map of the interaction between the two-within participant factors of Category and Presentation rate. An extensive left parietal region was identified. B) Volume maps of the 4 simple effects contrasting tools and animals at the different presentation rates. Talairach z-values correspond to locations that are typical of some of the landmarks of the tool network. Blue patches correspond to voxels that show stronger activations for tool than animals under 30 Hz, green patches correspond to voxels that show stronger activations for tool than animals under 15 Hz, red correspond to voxels that show stronger activations for tool than animals under 10 Hz, and purple correspond to voxels that show stronger activations for tool than animals under 5 Hz. All maps thresholded at FDR $q < .05$. C) This parietal region was further studied in order to understand whether high and low temporal frequency dependent tool-preferences were differentially distributed along the inferior-to-superior dimension. Thus, the left parietal interaction region was sliced in 3 mm planes along the z-dimension covering the area between $z = 31$ to $z = 61$ (y-axis in the plot). For each slice, the average *t*-values for tool-preferences for the two key temporal frequencies (5 and 15 Hz) were calculated and subtracted such that positive values on the x-axis indicate higher *t*-values for the low temporal frequency tool-specific contrast than for the high temporal frequency one, whereas negative values on the x-axis indicate higher *t*-values for the high temporal frequency tool-specific contrast than for the low temporal frequency one. IPS – Intraparietal sulcus; SMG – Supramarginal gyrus; AG – Angular gyrus.

Figure 2. Temporal frequency dependent tool-preferences in parietal cortex. Tool preferring regions within parietal cortex for different temporal frequency profiles. A) We present two contrasts: $Tools_{[5Hz]} > Animals_{[5Hz]}$ (colored purple) and $Tools_{[15Hz]} > Animals_{[15Hz]}$ (colored green; both maps: $q < .05$, FDR corrected). We then overlaid our low and high

temporal frequency tool-preferring regions on: B) the interaction region presented in Figure 1A; C) the parcellations proposed by Caspers and colleagues (2006), of the left inferior parietal lobule (BA 40); D) the parcellations of the intraparietal sulcus proposed by Choi et al.(2006), and Scheperjans et al. (2008a; 2008b); and E) the parcellations proposed by Scheperjans et al. (2008a; 2008b) for the superior parietal lobule (BA 7). Those parcellations were based on the SPM Anatomy Toolbox (Eickhoff et al., 2005).

Figure 1.

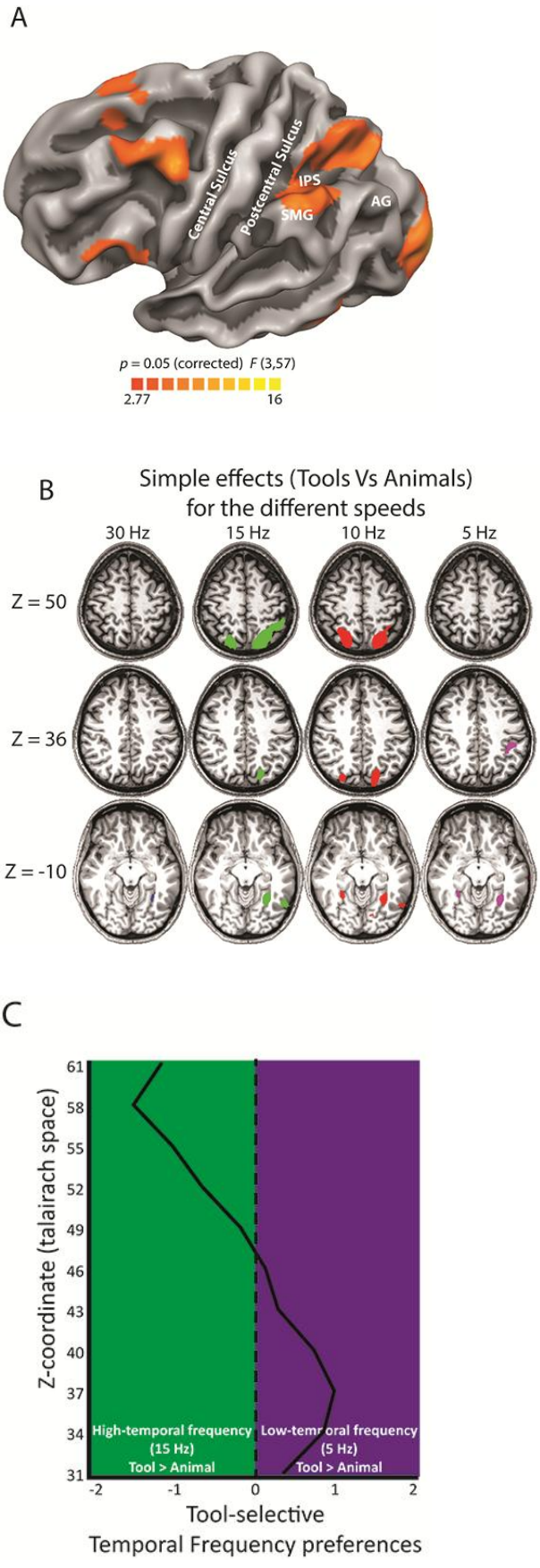
A
Central Sulcus
Postcentral Sulcus
IPS
SMG
AG
p = 0.05 (corrected) F (3,57)
2.77
16
B
Simple effects (Tools Vs Animals)
for the different speeds
30 Hz
15 Hz
10 Hz
5 Hz
Z = 50
Z = 36
Z = -10
C
Z-coordinate (talairach space)
61
58
55
52
49
46
43
40
37
34
31
High-temporal frequency
(15 Hz)
Tool > Animal
Low-temporal frequency
(5 Hz)
Tool > Animal
-2
-1
0
1
2
Tool-selective
Temporal Frequency preferences

Figure 2.

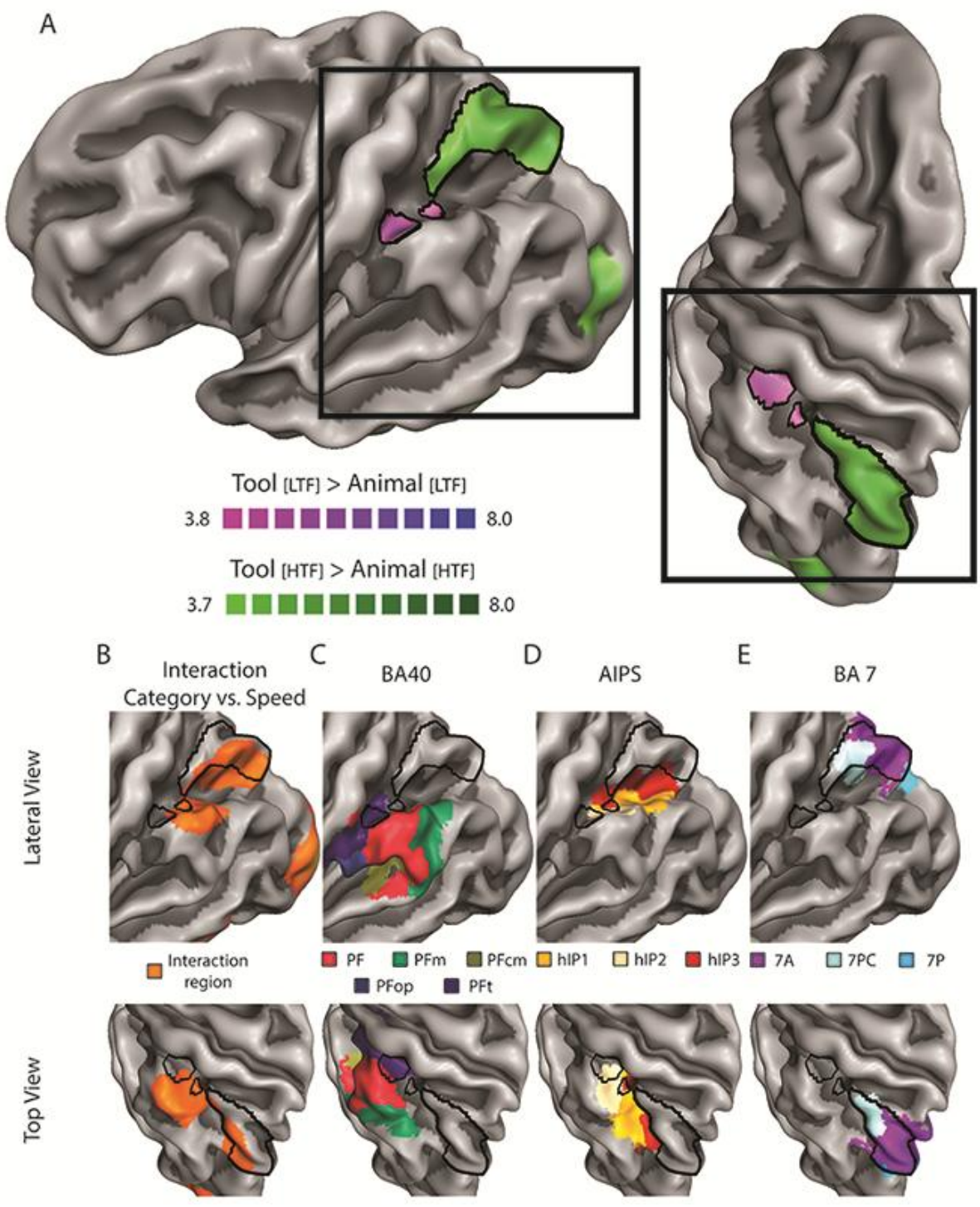
A
Tool [LTF] > Animal [LTF]
3.8
8.0
Tool [HTF] > Animal [HTF]
3.7
8.0
B
Interaction
Category vs. Speed
C
BA40
D
AIPS
E
BA 7
Lateral View
Top View
Interaction region
PF
PFm
PFcm
hIP1
hIP2
hIP3
7A
7PC
7P
PFop
PFt